A&A 396, L11–L15 (2002)
DOI: 10.1051/0004-6361:20021611

Astronomy & Astrophysics

Letter to the Editor

The warm-hot intergalactic medium at $z \sim 2.2$: Metal enrichment and ionization source⋆

J. Bergeron[1], B. Aracil[1], P. Petitjean[1,2], and C. Pichon[3]

[1] Institut d'Astrophysique de Paris - CNRS, 98bis Boulevard Arago, 75014 Paris, France
[2] LERMA, Observatoire de Paris, 61 Avenue de l'Observatoire, 75014 Paris, France
[3] Observatoire Astronomique de Strasbourg, 11 rue de l'Université, 67000 Strasbourg, France

Received 10 October 2002 / Accepted 31 October 2002

Abstract. Results are presented for our search for warm-hot gas towards the quasar Q 0329−385. We identify ten O VI systems of which two are within 5000 km s^{-1} of $z_{\rm em}$ and a third one should be of intrinsic origin. The seven remaining systems have H I column densities $10^{13.7} \leq N({\rm H\,I}) \leq 10^{15.6}$ cm^{-2}. At least ∼1/3 of the individual O VI sub-systems have temperatures $T < 1 \times 10^5$ K and cannot originate in collisionally ionized gas. Photoionization by a hard UV background field reproduces well the ionic ratios for metallicities in the range $10^{-2.5}$−$10^{-0.5}$ solar, with possibly sub-solar N/C relative abundance. For [O/C] = 0, the sizes inferred for the O VI clouds are in some cases larger than the maximum extent implied by the Hubble flow. This constraint is fulfilled assuming a moderate overabundance of oxygen relative to carbon. For a soft UV ionizing spectrum, an overabundance of O/C is required, [O/C] ≈ 0.0−1.3. For a hard(soft) U spectrum and [O/C] = 0(1), the O VI regions have overdensities $\rho/\overline{\rho} \approx 10$−40.

Key words. cosmology: observations – intergalactic medium – galaxies: halos – quasars: absorption lines

1. Introduction

Numerical simulations suggest the existence of a warm-hot phase in the intergalactic medium, $10^5 < T < 10^7$ K, which comprises a fraction of the baryons increasing with time. This phase should be mostly driven by shocks, at least at low redshift z (Cen & Ostriker 1999; Davé et al. 2001). Possible signatures of the warm-hot intergalactic medium (WHIM) are absorptions by high ionization species such as O V, O VI and O VII. These absorptions are difficult to detect as they either fall in the Lyα forest (below the atmospheric cut-off for $z < 1.92$) or in the soft X-ray range. Successful observations of the WHIM at low z were made with the FUSE, HST and Chandra satellites (e.g. Tripp et al. 2001; Savage et al. 2002; Nicastro et al. 2002).

At $z \sim 2$−2.5, an analysis of the O IV/O V ratio from HST stacked spectra favors a hard UV background spectrum (thus a small break at 4 Ryd) and the inferred metallicity is [O/H] $\simeq -2.2$ to -1.3 together with an enhanced oxygen abundance relative to carbon (Telfer et al. 2002). Detection of individual O VI absorbers has been recently reported: for systems at $z \sim 2.5$ with $N({\rm H\,I}) \sim 10^{14.0}$ to $10^{15.0}$ cm^{-2}, the inferred metallicity is [O/H] ~ -3 to -2 (Carswell et al. 2002) and for $N({\rm H\,I}) \geq 10^{15.5}$ cm^{-2} the metallicity is higher, [O/H] ≥ -1.5 (Simcoe et al. 2002). The main heating process of the high z WHIM is still unclear: the more tenuous regions of the Lyα forest could be ionized by a hard UV background spectrum, whereas the high column density population could be shock heated.

A systematic, large survey of quasar absorption lines at high S/N and high spectral resolution is being completed at ESO for a sample of about 20 quasars of which half are at $z \leq 2.6$. In this paper, we present the results of our search for O VI absorbers towards one quasar of the ESO large programme, Q 0329−385, with several unambiguous cases of narrow, strong and weak O VI absorptions. The observations, the selection procedure for O VI systems and our O VI sample are presented in Sect. 2. The constraints derived from the line widths are given Sect. 3. Our modelling of the O VI absorbers is presented in Sect. 4. The summary and conclusions are given in Sect. 5.

2. Observations and the O VI sample

The quasar Q 0329−385 ($z_{\rm em} = 2.423$) was observed at the VLT with the UVES spectrograph. The full wavelength coverage 3050–10 400 Å was obtained in two settings, using dichroics, with an exposure time of 6 hr per setting. The S/N ratio is about 30 and 100 at 3300 and 5000 Å respectively. The resolution is $b = 6.6$ km s^{-1}. A modified version of the ESO-UVES pipeline was used, better adapted to quasar spectra. A full description of the data reduction

Send offprint requests to: J. Bergeron, e-mail: bergeron@iap.fr

⋆ Based on observations made at the European Southern Observatory (ESO), under prog. ID No. 166.A-0106(A), with the UVES spectrograph at the VLT, Paranal, Chile.

Table 1. Column densities of the O VI systems in Q 0329−385.

z	n^a	H I	O VI	N V	C IV	Si IV
2.0615	1	14.26[d]	13.13	<12.30	<12.30	
2.0764	1	13.71	13.18	12.89	13.23	11.50[g]
2.1470	3	14.70	14.03	<12.60	<12.30	
2.2488	5	14.00[b]	14.29	<12.60	12.83[b]	
2.2515	4[f]	15.59	14.80	13.20	14.43[e]	12.71
2.3139	3	14.23	13.46	<12.50	12.45[c]	
2.3521	1	13.08	14.04	13.78	13.76	
2.3638	2	14.84	13.77	12.00[g]	12.53	
2.3729	3	15.24[e]	14.25	<12.50	12.69[c]	
2.4062	2	14.03	13.27	<12.30	<11.70	

[a] Number of individual O VI components. Ions spanning the same velocity range but with a different number of components are marked: [b] −2, [c] −1, [d] +1, [e] +2.
[f] Main complex.
[g] 2σ detection.

Table 2. Column densities of individual O VI sub-systems.

z(O VI)	H I	O VI	N V	C IV	Si IV
$\lvert\Delta z^a\rvert$	b	b	b	b	b
2.24835	12.87	13.63	<12.00	12.21	
4.1×10^{-5}	21.8	8.8		8.9	
2.25147	14.97	14.37	13.00	14.07	12.43
6.0×10^{-5}	18.0:	10.7	9.5	11.9	16.5
2.31395	13.90	13.20	<12.30	11.98	
0.8×10^{-5}	29.2	13.4		8.6	
2.35214[b]	13.08	14.04	13.78	13.76	
5.7×10^{-5}	21.8	12.7	9.6	9.1	
2.36385	14.55	13.50	12.00[c]	12.33	
6.3×10^{-5}	27.5	9.5		10.9	

[a] Difference between the redshifts of O VI and C IV.
[b] Intrinsic system.
[c] 2σ detection.

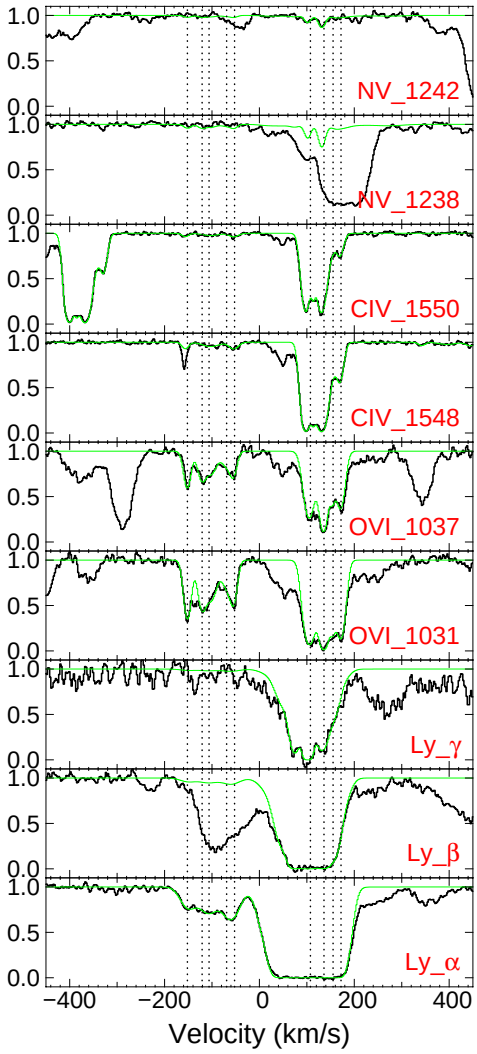

Fig. 1. The complex systems at $z = 2.2488$ and 2.2515. The thin line shows the best fit model only for the lines associated with the two O VI main clusters; there are additional components in the velocity range between these two clusters. The line blended with C IV1548 at $z = 2.24835$ is Mg I at $z = 0.76273$.

method will be presented in a forthcoming paper (Aracil et al. in preparation). The absorption lines were fitted by multiple Voigt profiles using the VPFIT software package (see `http://www.ast.cam.ac.uk/~rfc/vpfit.html`).

To identify the O VI systems, we used the following criteria: either the two lines of the doublet are clearly seen or, when one line of the doublet is partly blended, the presence of this line is clearly indicated by a distinct structure within the blend. In all cases, there are H I Lyman lines associated with the O VI doublets (see Table 1).

Our sample comprises ten O VI systems of which two within $\Delta v = 5000$ km s^{-1} of the quasar redshift. The redshift, number of components used in the fit and total column densities are given in Table 1. The range of N(H I) and N(O VI) covered by these systems overlap with those of the samples of Carswell et al. (2002) and Simcoe et al. (2002). The 3σ detection limits for individual sub-systems are typically (12, 2.0 and 1.0) $\times 10^{12}$ cm^{-2} for O VI, N V and C IV respectively. When C IV is detected, the upper limits for N V are estimated using the same number of components and same b values as for the C IV absorptions. When neither N V nor C IV is detected, we assume $b = 10$ km s^{-1} and a number of components equal to those of O VI.

The individual sub-systems for which a detailed modelling is presented in Sect. 4 have clean O VI doublets with little blending which ensures a correct estimate of the b parameter. The velocity shift between the O VI and C IV doublets is always small, $\leq$5.7 km s^{-1}, and usually larger than that between the O VI and Lyman lines. This was already noted by Rollinde et al. (2001). The column densities and b values are presented in Table 2. The stacked velocity plots are given only for the three intervening O VI systems with low b parameters.

3. Temperature

The histogram of the b(O VI) values is shown in Fig. 3 for the 25 individual components of the ten systems presented in Table 1, of which five are at $\Delta v < 5000$ km s^{-1} (shaded area).

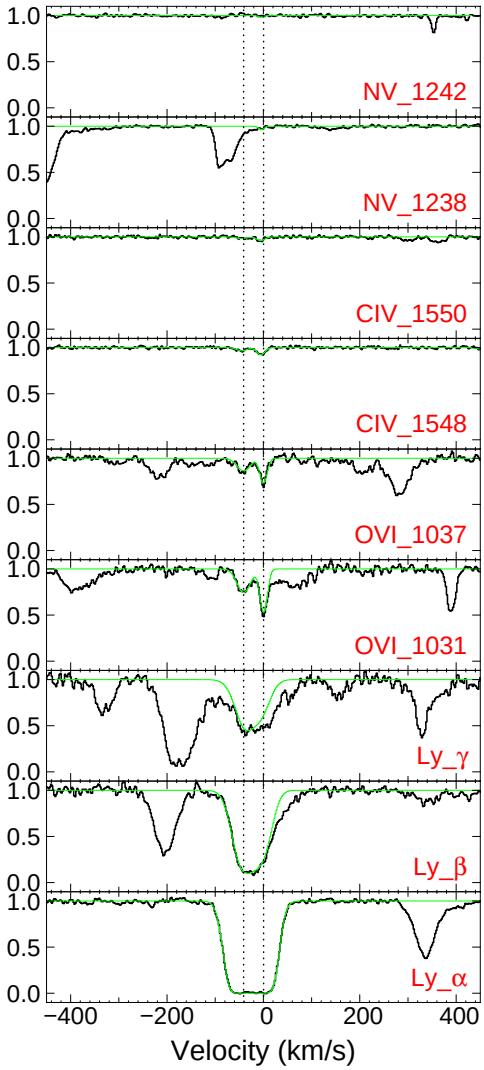

Fig. 2. The system at $z = 2.3638$ and the best fit model.

Seven (12) systems have line widths $b < 10(14)$ km s^{-1}, thus a temperature $T \leq 1.0(2.0) \times 10^5$ K. In the assumption of pure collisional ionization, this would imply $6.3 \times 10^{-8} \leq$ O VI/O $\leq 2.1 \times 10^{-2}$ (Sutherland & Dopita 1993) and very high oxygen abundances. At $T = (1.0, 1.5$ and $2.0) \times 10^5$ K, the values of [O/H] are log(O VI/H I)+(5.6,1.5,−0.7) respectively. For the systems and sub-systems given in Tables 1 and 2 log(O VI/H I) is $\gtrsim -1.0$. Consequently, the seven individual absorbers with $T \leq 1.0 \times 10^5$ K would have a metallicity [O/H] ≥ 4.6, i.e. oxygen would be the more abundant element log(O/H) ≥ 1.5. This clearly rules out collisional ionization for O VI absorbers with $b \leq 10$ km s^{-1}.

In addition the small velocity widths constrain the size of the absorbers. At $z \sim 2.2$, the line broadening due to the Hubble flow implies a maximun pathlength $l_{\rm H} = 80\, b_{10}$ kpc, assuming $H_0 = 65$ km s^{-1} Mpc^{-1}, $\Omega_{\rm M} = 0.3$ and $\Omega_\Lambda = 0.7$. In Sect. 4.2, this value is compared to the size of the absorbers based on the gas density derived from photoionization models in order to constrain the spectral energy distribution (SED) of the UV background spectrum.

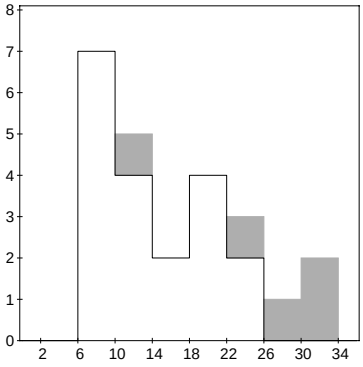

Fig. 3. Histogram of the b values of individual sub-systems.

4. Analysis of the O VI systems

Different SEDs were used for the UV background radiation at $z \sim 2.2$. The first one is a simple analytic fit to the spectrum given by Haardt & Madau (1996: hereafter HM96) with an energy spectral index $\alpha = 1.5$ ($f_\nu \propto \nu^{-\alpha}$) shortwards of 1 Ryd, a break of $10^{0.5}$ at 4 Ryd and adopting their normalization of the ionizing continuum at 1 Ryd. We also consider the spectrum derived by Madau et al. (1999: hereafter MHR99) which is softer with a stronger break ($10^{1.4}$) at 4 Ryd. Note that the analyses of He II/H I (Kriss et al. 2001), O IV/O V (Telfer et al. 2002) and O VI/C IV (Carswell et al. 2002) suggest a hard ionizing spectrum similar to that of HM96.

4.1. The oxygen abundance

We used the CLOUDY code (Ferland et al. 1998) to derive the ionization levels of the different species and their column density ratios. Results are given for optically thin systems, [C/H] = −1 and solar relative abundances. The ionization balance is very similar for any other values of [C/H] < -1 as the temperature, thus ionic ratios, is not strongly dependent on metallicity. Figure 4 gives N(O VI)/N(H I) ≡ O VI/H I as a function of N(O VI)/N(C IV) ≡ O VI/C IV. Variation of the metallicity results in a vertical shift of the theoretical curves. One system ($z = 2.3521$ and O VI/H I = 9.1) is clearly different from the rest of the absorbers: its metallicity should be about solar which strongly suggests an intrinsic origin. The presence of strong N V associated absorption reinforces this conclusion. For the other systems, their positions relative to the theoretical curves imply metallicities in the range [C/H] ≈ -0.5 to -2.5 for the harder ionizing spectrum.

The column density ratios of high ions is shown in Fig. 5. There is a single, well defined locus for the theoretical models with three different SEDs (HM96, MHR99 and our simple analytic fit to the HM96 spectrum with a break of $10^{1.0}$) and solar relative abundances. Two systems, with detected O VI, N V and C IV doublets, lie below this locus. The furthest away is the above mentioned, intrinsic system: the inferred sub-solar [O/N] abundance ratio is indeed consistent with the elemental abundances (enhanced nitrogen abundance relative to solar ratios) typical of most intrinsic absorbers (Hamann 1997). For four out of the other five systems with detected O VI

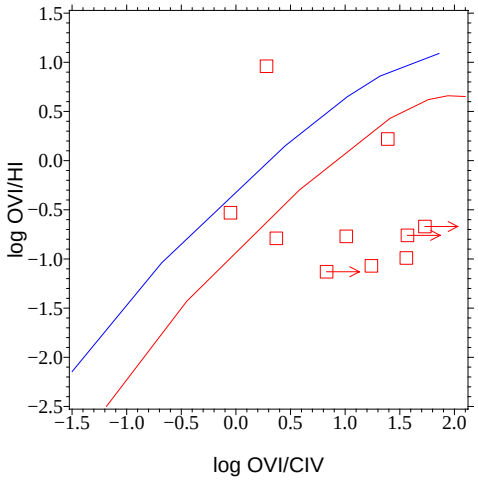

Fig. 4. The O VI/H I ratio versus O VI/C IV. The red and blue lines show the ratios obtained with the HM96 and MHR99 spectra respectively, [C/H] = −1.0 and solar relative abundances. The squares are the observed values for the ten systems given in Table 1 and upper limits are indicated by arrows.

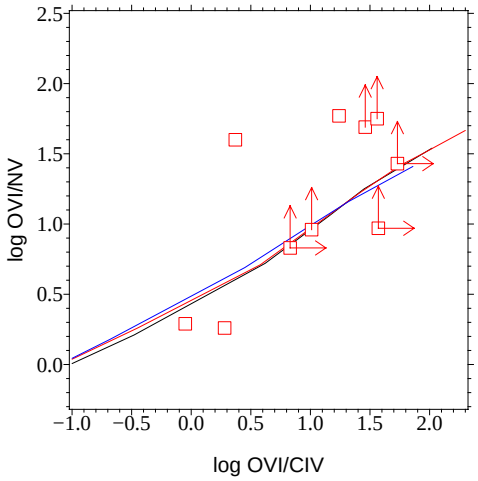

Fig. 5. The O VI/N V ionic ratio versus that of O VI/C IV. The red and blue lines refer to the same models as in Fig. 4 and, for the black one, the spectral slope $\alpha = 1.5$ and the break at 4 Ryd equals $10^{1.0}$. The other symbols are as in Fig. 4.

and C IV doublets, the observed ionic ratios imply either a super-solar [O/C] abundance ratio, as also found by Telfer et al. (2002) for WHIM clouds, and/or a sub-solar [N/C] abundance ratio.

4.2. Pathlength and abundances of some individual sub-systems

For each system the ionization parameter, U, is determined from O VI/C IV adopting a HM96 spectrum and solar relative abundances (Model A: see Fig. 6 and Table 3); the pathlength is derived from the modelled physical state of the gas. For the three sub-systems with O VI/H I > 0.1, one with N(H I) > 1×10^{15} cm^{-2}, the inferred sizes are compatible with limits given by the Doppler parameters (see Sect. 3) for a HM96 ionizing spectrum and solar relative abundances; the temperature

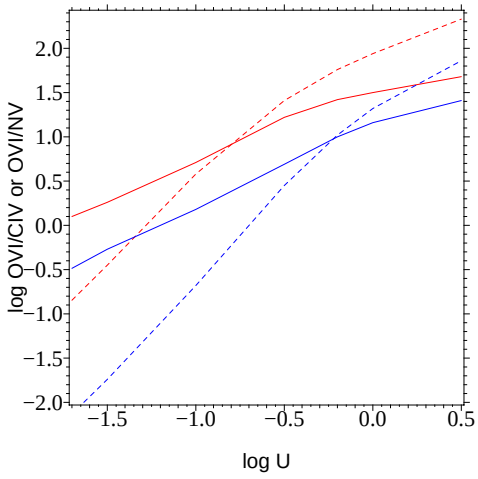

Fig. 6. The O VI/C IV (full lines) or O VI/N V (dotted lines) ionic ratio versus the ionization parameter U. Red and blue lines refer to the HM96 and MHR99 spectrum respectively together with solar relative abundances.

is $T = (3.0, 3.0 \text{ and } 4.8) \times 10^4$ K for the $z = 2.24835$, 2.25147 and 2.31395 absorbers respectively. However, for the $z = 2.36385$ sub-system with O VI/H I < 0.1, the inferred size is a factor ∼2 larger than the maximun size due to Hubble expansion; to have $l/l_{\rm H} \leq 1$ implies [O/C] $\gtrsim 0.3$.

A second model is then investigated assuming a HM96 spectrum and [O/C] = 1.0 (Model B). The derived ionization parameters are ∼3 times lower and $l \ll l_{\rm H}$ for all the individual sub-systems. Finally, since softer spectra imply higher U values, thus lower densities and larger pathlengths, we consider a MHR99 spectrum only together with [O/C] = 1.0 (Model C). Results for Models A and C are very similar as the decrease in U due to the enhanced [O/C] relative abundance (see Sect. 4.1) is compensated by the increase in U required by the larger break at 4 Ryd in the softer spectrum. The range in metallicity of the WHIM absorbers presented in Table 3 is [C/H] ∼ −0.7 to −2.9.

The constraints on the SED of the background ionizing spectrum and the [O/C] relative abundance are thus linked. Even for an ionizing spectrum as hard as the HM96 one, we find that there must be some O VI clouds with a super-solar [O/C] relative abundance. Adopting the MHR99 soft spectrum implies [O/C] ≈ 0.0 to 1.3.

Note that in the $z = 2.25147$ absorber, a fraction of C IV could reside in the Si IV phase. Using O VI/N V instead to derive U, with [O/N] = 0 and adopting the HM96 spectrum, gives $l \simeq 1$ Mpc, inconsistent with the Hubble expansion constraint. The latter is fulfilled for [O/N] ≥ 0.7.

5. Summary and conclusions

A sample of ten O VI absorption systems at $z = 2.06$–2.41 was identified in Q 0329−385. Seven systems trace the warm-hot intergalactic medium, outside the close neighbourhood of the quasar. All the detected intervening O VI systems have associated H I absorption with column densities in the range $10^{13.7}$–$10^{15.6}$ cm^{-2}. At least ∼1/3 of the individual

Table 3. Abundances and pathlength of the O VI absorbers.

z(O VI)	M^a	[N/C]	U	H/H I	l(kpc)^b	[C/H]
2.24835	A	<–0.43	−0.50	5.21	6.5	−0.67
	B	<–0.05	−1.05	4.58	0.4	−0.84
	C	<0.03	−0.50	5.21	6.5	−1.39
2.25147	A	−0.76	−1.08	4.55	47.0	−1.13
	B	−0.18	−1.60	3.98	3.8	−0.90
	C	−0.22	−1.05	4.58	54.0	−1.45
2.31395	A	<0.21	−0.63	5.07	37.0	−2.00
	B	<0.63	−1.18	4.45	2.5	−2.00
	C	<0.68	−0.60	5.10	43.0	−2.65
2.36385	A	~–0.45	−0.66	5.03	141.0	−2.31
	B	~0.01	−1.22	4.41	9.3	−2.28
	C	~0.02	−0.64	5.05	155.0	−2.92

[a] Model A: $\alpha = 1.5$, log(He II break) = 0.5, [O/C] = 0.0, Model B: $\alpha = 1.5$, log(He II break) = 0.5, [O/C] = 1.0, Model C: Madau et al. (1999), [O/C] = 1.0.
[b] Hubble flow constraint: $l_{\rm H} \leq 80\, b_{10}$ kpc.

O VI subcomponents have low velocity dispersions, $b < 10$ km s^{-1}. These unambiguous cases of low temperature, $T < 1 \times 10^5$ K, imply a radiative ionizing process for the tenuous regions of the WHIM.

The observed O VI/H I and O VI/C IV ionic ratios are well reproduced by photoionization models with a hard (HM96) spectrum and [O/C] = 0, whereas the weakness or non detection of N V implies [O/N] > 0 in most cases. The range in metallicity for our small sample is large, [C/H] ≈ -0.5 to -2.5, which strongly suggests a non-uniform enrichment of the intergalactic medium. The size inferred for low b absorbers of smaller O VI/H I ratios are about twice as large as that inferred from the Hubble flow constraint. For these absorbers, higher gas densities, thus sizes compatible with the Hubble flow, are obtained for [O/C] ~ 0.3.

An enhanced oxygen abundance is nearly always required for a softer spectrum (i.e. a larger break at 4 Ryd), with [O/C] $\approx$ 0.0−1.3, and the enrichment of the WHIM should then comes predominantly from massive stars. Adopting the MHR99 spectrum and [O/C] = 1 leads to a metallicity range [C/H] ≈ -1.2 to -3.0.

The N(H I) range of the O VI systems in Q 0329−385 is similar to that of the O VI sample of Carswell et al. (2002) and these authors also favor photoionization of the WHIM. They rule out a soft UV flux for a solar [O/C] abundance ratio, as also found for most of the O VI systems in Q 0329−385 but, as discussed in Sect. 4.2, a softer UV flux is acceptable if [O/C] is super-solar. On the contrary, Simcoe et al. (2002) favor shock-heated gas. However, their O VI survey does not trace regions of lower column densities (no system with N(H I) $< 1 \times 10^{14.5}$ cm^{-2}) and five out of their 12 intervening O VI absorbers have very large N(H I) ($10^{16.9}$ to $10^{19.5}$ cm^{-2}). The O VI systems with stronger H I absorption may trace the outer parts of high z galatic halos where the effects of galactic winds may dominate the heating process (Theuns et al. 2002), one of the models also suggested by Simcoe et al. (2002).

For a hard UV spectrum and [O/C] = 0, the gas density is in the range $n_{\rm H} = (7{-}23) \times 10^{-5}$ cm^{-3}, thus O VI arises in regions with overdensities $\rho/\overline{\rho} \approx 10{-}40$ for $\Omega_{\rm b} h^2_{100} = 0.02$ (O'Meara et al. 2001). Adopting a MHR99 soft spectrum and [O/C] = 1 leads to the same range of overdensities, whereas for the HM96 spectrum and [O/C] = 1 the overdensities are about three times larger.

We are currently building a large O VI sample from the dataset of the VLT-UVES quasar large programme to investigate the physical state and chemical evolution of the O VI absorber populations, as well as the relative occurence of O VI and C IV systems.

Acknowledgements. We are grateful to R. Carswell for stimulating discussions and his assistance with the VPFIT s/w code.

References

Carswell, B., Schaye, J., & Kim, T.-S. 2002, ApJ, 578, 43
Cen, R., & Ostriker, J. P. 1999, ApJ, 514, 1
Cowie, L. L., Songaila, A., Kim, T.-S., & Hu, E. M. 1995, AJ, 109, 1522
Davé, R., Cen, R., Ostriker, J. P., et al. 2001, ApJ, 552, 473
Ferland, G. J., Korista, K. T., Verner, D. A., et al. 1998, PASP, 110, 761
Haardt, F., & Madau, P. 1996, ApJ, 461, 20
Hamann, F. 1997, ApJS, 109, 279
Kriss, G. A., Shull, J. M., Oegerle, W., et al. 2001, Science, 293, 1112
Madau, P., Haardt, F., & Rees, M. J. 1999, ApJ, 514, 648
Nicastro, F., Zezas, A., Drake, J., et al. 2002, ApJ, 573, 157
O'Meara, J. M., Tytler, D., Kirkman, D., et al. 2001, ApJ, 552, 718
Rollinde, E., Petitjean, P., & Pichon, C. 2001, A&A, 376, 28
Savage, B. D., Sembach, K. R., Tripp, T. M., & Richter, P. 2002, ApJ, 564, 631
Simcoe, R. A., Sargent, W. L. W., & Rauch, M. 2002, ApJ, 578, 737
Songaila, A., & Cowie, L. L. 1996, AJ, 112, 335
Sutherland, R. S., & Dopita, M. A. 1993, ApJS, 88, 253
Telfer, R. C. , Kriss, G. A., Zheng, W., Davidsen, A. F., & Tytler, D. 2002, ApJ, in press [astro-ph/0207301]
Theuns, T., Viel, M., Kay, S., et al. 2002, ApJ, 578, L5
Tripp, T. M., Giroux, M. L., Stocke, J. T., Tumlinson, J., & Oegerle, W. R. 2001, ApJ, 563, 724
Tytler, D., Fan, X.-M., Burles, S., et al. 1995, in QSO Absorption Lines, ed. G. Meylan (Berlin: Springer), 289